Innovation in environmental sustainability: carbon credits with proof of reserve on rural properties according to the standards of regulated markets

Innovation in environmental sustainability: carbon credits and the rural reserve

Marcos Alexandre Fernandes Ferronato[1,¶*], Ana Carolina Clivatti Ferronato[2¶], Miguel Angel Uribe Opazo[1¶]

[1] Programa de Pós-graduação em Engenharia Agrícola – PGEAGRI, Universidade Estadual do Oeste do Paraná - UNIOESTE, Campus Cascavel, Cascavel, Paraná, Brasil.

[2] Programa de Pós-Graduação em Desenvolvimento Rural Sustentável – PPGDRS, Universidade Estadual do Oeste do Paraná - UNIOESTE, Campus de Marechal Cândido Rondon, Marechal Cândido Rondom, Paraná, Brasil.

[*] Corresponding author

E-mail: ferronato@networdtecnologia.com

[¶]These authors contributed equally to this work

Abstract

Farms are increasingly recognized as carbon sinks with significant potential to mitigate climate change. This study documents how farms can become positive climate assets by using portable sensors, satellite imagery, blockchain, and AI to quantify and monetize carbon removal. This technological integration enables the issuance of traceable and secure carbon credits, promoting sustainable land use and granting a range of farms access to the carbon markets. We evaluated the reliability and spatial consistency of soil carbon retention in agricultural and forestry systems on four rural properties in Brazil during the 2022/2023 harvest. Using a protocol certified by the Brazilian legislation, we compared sensor-derived carbon estimates with reference measurements in farmland and forest areas. In agricultural areas, sensor readings showed high agreement with reference standards, reflecting strong adherence to certified standards. Agreement was more heterogeneous in forested areas, suggesting spatial variations in carbon stocks not captured by conventional methods. Spatial analysis revealed distinct patterns of autocorrelation between land use types, with stronger spatial clustering in agricultural systems. The results demonstrate that proprietary sensors integrated with artificial intelligence platforms are effective for estimating carbon retention, especially in cultivated areas, and offer great potential for supporting the certification of carbon credits based on auditable data. The results also highlight the effectiveness of land management practices and the potential of forest and agricultural areas as legitimate sources of regulated carbon credits. These credits can serve as effective tools for the transition to a low-carbon economy, especially in sectors with higher difficulty in reducing emissions. In addition, they promote social and climate justice by linking the carbon sequestration potential of the global South with the North's demand for compensation, providing environmental, economic, and social benefits.

Introduction

Rural properties have been increasingly recognized not only as essential sources of food and fiber, but also as important carbon sinks, with significant, though still underutilized, potential to mitigate climate change [1, 2]. By measuring greenhouse gas (GHG) removals and equivalent carbon stocks in legally reserve areas and consolidated agricultural zones, this research robustly documents how rural properties can be transformed into valuable positive climate assets [3]. This system builds the technical and institutional infrastructure needed for effective and sustainable emissions mitigation, while strengthening the environmental, social, economic, and governance (ESG) dimensions of sustainability [4]. Notably, these innovations offer an inclusive and equitable pathway for rural communities of any size to actively participate in global carbon markets, helping to bring climate policies closer to local realities [5].

In a scenario of strong innovation, soil monitoring is conducted by proprietary portable sensors based on electrical conductivity, which allow precise measurement of soil physical and chemical characteristics, as well as carbon retention in agricultural and forest soils [6]. To complement this approach, high-resolution satellite images provide crucial data on the carbon stored in forest and crop areas, as well as on emissions from agricultural management practices [7]. The integration of these data sources allows for detailed and reliable quantification, facilitating the issuance of tokenized, proof-of-stock carbon credits that meet the strict integrity and transparency criteria required by regulated markets. This framework goes beyond a mere technical solution, becoming a transformative mechanism for the transition towards more sustainable land use [8]. With growing global climate finance, rural areas in the global south have the potential to play a key role not only in mitigating emissions but also in ecological restoration, protecting biodiversity, and promoting climate justice. By overcoming technical, financial, and operational barriers that have historically excluded small and medium-sized farms from carbon markets [9], this system offers these farms an opportunity to participate through a replicable model that guarantees reliability, transparency and transparency.

[10] had already highlighted the need for offset schemes that encourage landowners to join carbon credit programs, while [11] reinforced the importance of certifications to ensure ethical and socially responsible offsets. Recent studies also point out that an efficient market requires both transparent data structures and decentralized verification systems that ensure compliance and trust in the offsets offered [12, 13].

Faced with the urgency of the climate crisis, the limitations of voluntary carbon markets, often criticized for a lack of transparency and inconsistent methodologies, have come to light. Our approach seeks to overcome these limitations by strictly following the standards of regulated markets, offering a robust and reliable platform for both credit buyers and farmers. In doing so, we support the objectives of the Paris Agreement and respond to demands for fairer and more transparently allocated climate finance from developed countries [14].

In the context of this study, an innovative approach is presented that integrates advanced geospatial monitoring, proprietary sensors, artificial intelligence (AI), and blockchain certification to quantify and monetize carbon removal on rural properties. These synergistic technologies enable the generation of carbon credits that are highly traceable, secure, and comply with the stringent standards of global regulated markets. Ultimately, this research contributes to the development of a scalable, data-driven, ecosystem-integrated, and socially inclusive carbon credit system. By harnessing existing ecosystems in rural landscapes - especially agricultural soils and forests - it offers a solid pathway for countries seeking to achieve their emissions reduction targets, while promoting economic equity and environmental resilience in a sustainable and lasting way.

Material and methods

Study sites

This research project was conducted during the 2022/2023 summer harvest, covering soybean and corn crops on four rural properties located in the state of Paraná, Brazil. The selected areas adopt the no-till system and vary in soil type (clay and mixed), as described below: A) Agropecuária Vanguarda property - Located in the municipality of Cascavel (PR), it has predominantly clay soil and a no-till system. The total area of the rural property is 292.89 hectares, with geographical coordinates of the centroid at 24°94'53.47“ S and 53°52'98.15” W. During the 2022/2023 summer harvest, soybeans were grown. B) Smart Farm property - Located in the municipality of Toledo (PR), it also has clay soil and adopts the no-till system. The property has a total area of 24.04 hectares, with centroid coordinates at 24°62'70.80“ S and 53°70'89.99” W. Soybeans were grown in the 2022/2023 summer harvest. C) Perpétuo Socorro property - This property is located in the municipality of Campina da Lagoa (PR), with mixed soil characteristics and no-till management. The total area of the rural property is 205.65 hectares, with centroid coordinates at 24°74'51.17“ S and 52°86'85.87” W. Corn was grown during the 2022/2023 summer harvest. D) Bela Vista property - Also located in the municipality of Campina da Lagoa (PR), it has mixed soil and uses the no-till system. The property covers 88.61 hectares, and its centroid is located at coordinates 24°67'54.56“ S and 53°88'02.73” W. In the summer of 2022/2023, the crop planted was soybeans (Fig. 1).

Figure 1. Properties studied with forest and crop areas.

Data acquisition and analysis

The methodology and technology implemented here can be used in extension crops (soybeans, corn, wheat, oats, rice, cotton, sugar cane, beans, among others), perennial crops (pasture, coffee, cocoa, mango, avocado, among others) and forest crops (pine and eucalyptus) in the Amazon rainforest, Atlantic rainforest, Cerradão, Cerrado, Pantanal, Caatinga and Várzea biomes. The framework used was applied to the four properties throughout seven harvests and followed the following steps to determine the carbon credits: a) Socio-environmental analysis - Initially, the properties were screened by checking the Rural Environmental Registry (CAR) and the Rural Property Registration Certificate (CCIR). It was ensured that the legal owners - natural or legal persons - had no records of work analogous to slavery or involvement in illegal deforestation, following current Brazilian legislation and the criteria of the EU Deforestation Regulation (EUDR); b) Origination - Carbon quantification was entirely sensor-based (100%), combining on-site measurements and remote sensing, considering: (1) Agricultural soil and forest soil: the equivalent carbon retained was measured with proprietary portable sensors based on electrical conductivity, duly certified. These measurements took place once per production cycle; (2) Crops and forests: carbon retention was monitored regularly throughout the agricultural cycle using satellite images; (3) Emissions associated with agricultural practices: stages such as soil preparation, planting, spraying, harvesting, transportation and complementary activities were monitored by satellite, allowing associated emissions to be calculated. Based on these measurements, carbon balances were made for each property (carbon emitted - carbon retained = net emissions). When net emissions were negative, equivalent carbon credits were generated; c) Structuring - The information generated in the previous stages was organized into a georeferenced technical document containing all the project specifications. This document was drawn up following the protocols of regulated carbon markets and the Greenhouse Gas Protocol (GHG Protocol); d) Certification - Certification of the carbon credits generated was carried out by an independent third party, duly accredited by the competent government authorities. This stage ensured the methodological and technological validity of the quantification and verification of the credit issued; e) Tokenization - Each ton of carbon equivalent effectively removed from the atmosphere resulted in the generation of a digital token, corresponding to a carbon credit. These tokens were issued on a public blockchain, with full traceability and proof of reserve (Real World Assets), guaranteeing security and transparency; f) Custody and Trading - The tokens were made available on a digital platform for trading via digital wallets. This infrastructure allowed the credits to be retired as and when they were used by companies to offset emissions, in compliance with regulated market legislation in different countries; g) Financial Operation - The entire process was supported by licensed financial operators, responsible for intermediating and validating transactions between producers and buyers of credits, ensuring compliance with legal requirements and the integrity of the assets transacted.

To carry out this research, specific tools and technologies were used to monitor, analyze, and model environmental and agronomic data. Soil analysis was carried out using a proprietary portable electrical conductivity sensor, developed by the author [15, 16], which combined with mathematical models and proprietary artificial intelligence software, made it possible to generate georeferenced maps with estimates of the chemical and physical composition and the amount of carbon retained in the soils of agricultural and forestry areas. Crop, pasture, and forest monitoring was carried out by processing free satellite images from the Landsat 8 and Sentinel-2 sensors, using mathematical models and proprietary artificial intelligence software [15, 16] to estimate the carbon retained in the vegetation cover and the carbon emitted during agricultural management, generating georeferenced maps of both variables. Statistical analyses were carried out using local and global Moran's indexes, applied to validate the conformity and geospatial consistency of the data on each property and between them [17]. The georeferenced visualization was carried out in the free software QGIS [18], using shapefile files with the values of carbon retained and emitted in each of the identified sinks. The models and algorithms developed, based on convolutional neural networks and integrated computer vision, were processed in a cloud computing environment using high-performance machines from the Google Cloud platform [19], ensuring adequate computing capacity, scalability, and efficiency in the generation of carbon equivalent retention and emission maps.

Mathematical modeling of retention and emission elements

The mathematical modeling involved the following steps (A-M), each of which was carried out with the support of AI software. This technology was separated into three layers. The first layer involved the hardware for capturing information from the soil in the fields and the soil in the forest (proprietary electrical conductivity sensor), satellite images of the fields and forests. In the second layer were the mathematical models of soil patterns (soil chemistry and physics, and retained carbon) and carbon retention patterns in forests and crops. In the third layer, AI software based on convolutional neural networks (CNN) was trained to identify the modeled patterns within the data set monitored by the sensors.

a) Carbon retained in soil (crops and forests)

The variable carbon retained in soil per monitored plot $Crs(t)$ represents the measurement made by the proprietary soil sensor used in this research, measuring the 0-30 cm soil layer. Based on the sensed information, the proprietary AI software used in this research generates the values of the soil carbon concentration, soil density, and soil biome textural class variables and calculates the carbon retained in soil using the previously modeled standards.

$$Crs(t) = \sum_{k=1}^{n} \left(\binom{n}{k} CM^{C}\right) * 2000 * \partial(|dens|/|cltex|) \quad (1)$$

where,

Crs → Carbon retained in the soil;

n → total number of carbon concentration spots in the plot;

t → monitored plot;

CM^C → average carbon concentration measured at the point relative to the patch in which it is located;

dens → Soil density;

cltext → numerical representation of the soil textural class.

b) Carbon retained in forests

The carbon retained in forests variable per monitored plot $(Crf(t))$ represents the measurement made by the satellite image sensor used in this research, based on the top image of the trees in the monitored plot. From these images, the proprietary AI software used in this research generates the variables total number of hectares, identifies the type of biome, and calculates the carbon retained in the forest using the previously modeled patterns.

$$Crf(t) = \sum_{k=1}^{n} \binom{n}{k} Ckg^t bioma_1^7 * 2500 arvha\, \partial(img \int_4^{pg} var), \quad (2)$$

where,

Crf → Carbon retained in the forest first harvest;

n → total number of hectares;

t → monitored plot;

Ckg → Kilograms of carbon

bioma → biome of the plot (Atlantic Forest, Amazon biome, Cerradão, Cerrado, Caatinga, Várzea, Pantanal);

arvha → number of trees per hectare

img → georeferenced image

pg → georeferenced points

var → model calculation base

c) Carbon retained in crops

The variable carbon retained in crops per monitored plot, $CCult(a)$ represents the measurement made by the satellite image sensor used in this research, based on the top image of the plants in the monitored plot. From these images, the proprietary AI software used in this research generates the variables total number of hectares, identifies the type of crop, and calculates the carbon retained in the crop using the previously modeled patterns. Here, net values are considered, discounting the grain, fruit, or trunk of forestry trees that go for further processing and emit carbon.

$$CCult(a) = \sum_{k=1}^{n} \int_{4}^{mt} var\% \, (mt \, a_1^m) \begin{pmatrix} a11 & \cdots & a1n \\ \vdots & \ddots & \vdots \\ an1 & \cdots & ann \end{pmatrix} * ctr^{mt} * \%ppgg \quad (3)$$

where,

CCult(a) → Carbon retained in the crop (corn, soybean, wheat, beans, oats, cotton, sugarcane, and pasture);

a → modeled crops (short cycle and perennial cycle)

K → initial number of patches of concentration variation;

n → total number of patches of concentration variation;

m → minimum number of months in the crop cycle;

mt → maximum number of months in the crop cycle;

ctr → total carbon retained;

%ppgg → percentage variation in overall crop loss and gain in the plot;

var% → percentage variation in month m of the cycle about mt.

d) Carbon retained in the soil (crop and forest), second harvest

The carbon retained in the soil variable per plot monitored from the second harvest onwards represents the measurement performed by the proprietary soil sensor used in this research, with measurements in the 0-30 cm soil layer, from the second crop cycle onwards. Based on the sensor information, the proprietary AI software used in this research generates the values of the variables of soil carbon concentration, soil density, and soil biome textural class, and calculates the carbon retained in the soil using previously modeled patterns. After this measurement, the soil carbon measurement of the plot from the previous harvest is discounted.

$$Crs2(t) = \left(\sum_{k=1}^{n} \binom{n}{k} CM^{C} * 2000\right) * \partial(|dens|/|cltex|) - Crs(t) \quad (4)$$

where,

Crs2 → Carbon retained in the soil from the second harvest onwards;

n → total number of carbon concentration spots in the plot;

t → monitored plot;

CM^C → average carbon concentration measured in the patch;

dens → soil density;

Crs(t) → Measurement of carbon retained in the plot in the previous harvest;

cltext → numerical representation of the soil textural class.

e) Carbon retained in forests from the second harvest onwards

The variable carbon retained in forests from Second Harvest onwards per monitored plot $Crf2(t)$ represents the measurement made by the satellite image sensor used in this research, from the top image of the trees in the monitored plot. From these images, the proprietary AI software used in this research generates the variables total number of hectares, identifies the type of biome, and calculates the carbon retained in the Forest using previously modeled patterns.

After this measurement, the carbon measurement in the forest of the plot from the previous harvest is discounted.

$$Crf2(t) = \sum_{k=1}^{n} \left(\binom{n}{k} Ckg^{t} bioma_{1}^{7} * 2500 arvha\, \partial\left(img \int_{4}^{pg} var\right)\right) - Crf(t) \quad (5)$$

where,

Crf2 → carbon retained in the forest from the second harvest onwards;

n → total number of hectares;

t → monitored plot;

Ckg → kilos of Carbon

bioma → plot biome (Atlantic Forest, Amazon biome, Cerradão, Cerrado, Caatinga, Floodplain, Pantanal);

arvha → number of trees per hectare

img → georeferenced image

pg → georeferenced points

var → model calculation base

These values, determined by the models above, may be impacted by climate conditions, management conditions, and infestations of agents that cause damage. Based on this, the model proposed by the technology corrects the retention amounts according to the following impact elements.

f) Reduction in retained carbon in the crop about the volumes and frequency of rainfall

The variable of loss/gain of carbon retained in the crop was determined by plot with the volumes and frequency of rainfall $PGclP(t)$ represents the calculation performed by the proprietary AI software used by this research, based on the plot's rainfall index data with georeferenced historical data from INPE (National Institute for Space Research) [20], through its IAPs (Application Programming Interface) for access.

$$PGclP(t) = \int_1^5 (qc^{mm})^{+}_{-}\%pgp(fmm\ a_1^n)\begin{pmatrix} a11 & \cdots & a1n \\ \vdots & \ddots & \vdots \\ an1 & \cdots & ann \end{pmatrix} * pa \qquad (6)$$

where,

Pch → Total loss/gain of carbon retained in the crop concerning the volumes and frequency of rainfall;

t → monitored plot;

qc → amount of rainfall in millimeters;

%pgp → percentage variation of loss and gain in the reference month;

fmm → range of millimeters of rainfall;

a → matrix element of the range matrix;

n → index of the range matrix;

pa → target productivity.

g) Decrease in carbon retained in the field with soil correction actions

The variable loss/gain of carbon retained in the field was calculated by plot with the assertiveness and quality of soil correction $PGclC(t)$ represents the calculation carried out by the proprietary AI software used by this research, based on the chemical and physical analysis data carried out by the proprietary sensor used by this research and its respective georeferenced soil correction maps.

$$PGclC(t) = \int (rd^c)^{+}_{-}\%pgp_1^f(frd) * \mathrm{PGclP(t)} \qquad (7)$$

where,

PGclC → Crop loss or gain about soil correction management;

t → monitored plot;

rd → actual availability of soil correction;

%pgp → percentage variation in loss and gain from the reference range;

frd → actual availability range.

h) Decrease in carbon retained in the field with soil fertilization actions

The variable loss/gain of carbon retained in the field was calculated per plot with the assertiveness and quality of soil fertilization $PGclA(t)$ represents the calculation carried out by the proprietary AI software used by this research, based on the chemical and physical analysis data carried out by the proprietary sensor used by this research and its respective georeferenced soil fertilization maps.

$$PGclA(t) = \int (rd^{a})_{-}^{+}\%pgp_{1}^{f}(frd) * PGclC(t) \qquad (8)$$

where,

PGclA → Crop loss or gain about soil fertilization management;

t → monitored plot;

rd → actual availability of soil fertilization;

%pgp → percentage variation in loss and gain from the reference range;

frd → actual availability range.

i) Decrease in carbon retained in the field with pest management actions

The variable loss/gain of carbon retained in the field was calculated per plot with the assertiveness and quality of pest management $PGclMP(t)$ represents the calculation made by the proprietary AI software used in this research, based on the image data of the plots and their respective georeferenced pest infestation maps.

$$PGclMP(t) = \int (inf^{p})^{+}_{-}\%pgp_{1}^{f}(frd) * PGclA(t) \quad (9)$$

where,

PGclMP → Loss or gain of the crop about pest management;

t → monitored plot;

inf → % pest infestation;

%pgp → percentage variation in loss and gain of the reference range;

frd → infestation range.

j) Decrease in carbon retained in the field with disease management actions

The variable loss/gain of carbon retained in the field calculated by plot with the assertiveness and quality of disease management $PGclMD(t)$ represents the calculation made by the proprietary AI software used in this research, based on the image data of the plots and their respective georeferenced maps of disease infestation.

$$PGclMD(t) = \int \left(inf^{d}\right)^{+}_{-}\%pgp_{1}^{f}(frd) * PGclMP(t) \qquad (10)$$

where,

PGclMD → Loss or gain of the crop about the risk of disease management;

t → monitored plot;

inf → % disease infestation;

%pgp → percentage variation of loss and gain of the reference range;

frd → infestation range.

k) Decrease in carbon retained in the field with the incidence of solar radiation

The variable loss/gain of carbon retained in the field calculated by plot with the volumes and periodicity of solar radiation $PGclR(t)$ represents the calculation carried out by the proprietary AI software used in this research, based on the solar radiation index data of the plot with georeferenced historical data from INPE [20], through its access IAPs.

$$PGclR(t) = \int_{1}^{5} (rs^{mj}) \pm \%pgp(fmj\ a_1^n) \begin{pmatrix} a11 & \cdots & a1n \\ \vdots & \ddots & \vdots \\ an1 & \cdots & ann \end{pmatrix} * CCult(a) * \%ppgl \quad (11)$$

where,

PGclR → Loss gain total carbon retained in the crop by solar radiation;

t → monitored plot;

CCult(a) → Carbon retained in the crop (corn, soybeans, wheat, beans, oats, cotton, sugarcane, and pasture);

rs → solar radiation in megajoules per m2;

%pgp → percentage change in loss and gain in the reference month;

a → matrix element of the range matrix;

fmj → mega joule range of solar radiation.

l) Decrease in carbon retained in forests with the volume and frequency of rainfall

The variable loss/gain of carbon retained in the forest calculated by plot with the volume and frequency of rainfall $PGcfP(t)$ represents the calculation carried out by the proprietary AI software used in this research, based on the rainfall index data for the plot with georeferenced historical data from INPE [20], through its access IAPs.

$$PGcfP(t) = \int_1^5 (qc^{mm})^{+}_{-}\%pgp(fmm\ a_1^n)\begin{pmatrix} a11 & \cdots & a1n \\ \vdots & \ddots & \vdots \\ an1 & \cdots & ann \end{pmatrix} * pa \qquad (12)$$

where,

PGcfP → Loss gain total carbon retained in the forest by the volume and periodicity of rainfall;

t → monitored plot;

qc → amount of rainfall in millimeters;

%pgp → percentage variation in loss and gain in the reference month;

a → matrix element of the range matrix;

fmm → range of millimeters of rainfall;

pa → target productivity.

m) Decrease in carbon retained in the forest about the incidence of solar radiation

The variable loss/gain of carbon retained in the forest calculated by plot with the volumes and periodicity of solar radiation $PGcfR(t)$ represents the calculation carried out by the proprietary AI software used by this research, based on the plot's solar radiation index data with georeferenced historical data from INPE [20], through its access IAPs.

$$PGcfR(t) = \int_1^5 (rs^{mj})^{+}_{-}\%pgp(fmj\ a_1^n)\begin{pmatrix} a11 & \cdots & a1n \\ \vdots & \ddots & \vdots \\ an1 & \cdots & ann \end{pmatrix} * CCult(a) * \%ppgl \qquad (13)$$

where,

PGcfR → Loss gain total carbon retained in the forest by the incidence of solar radiation;

t → monitored plot;

CCult(a) → Carbon retained in the crop (corn, soy, wheat, beans, oats, cotton, sugarcane, and pasture);

rs → solar radiation in megajoules per m2;

%pgp → percentage change in loss and gain in the reference month;

%ppgf → percentage gains and losses in forest productivity;

a → matrix element of the range matrix;

fmj → mega joule range of solar radiation.

The analyses performed by the research took into account the following variables: carbon retained in the soil of the crop and its counter-evidence, carbon retained in the soil of the forest and its counter-evidence, carbon retained in the crop and its counter-evidence and carbon retained in the forest and its counter-evidence, and these are following the certification issued for the methodology and technology (issued by an independent third-party company accredited by the Brazilian government to perform such action – attached to this document), which determines a maximum margin of error of 5% (five percent).

To evaluate the global (Table 1) and local Moran indexes (Table 2), the relative variation rates represented in equation 14 were used, with the sensorized measurements and the counter-evidence measurements unified in a results table. These result tables, generated from the application of the relative variation rate between the two measurements (equation 14), will be the object of analysis of the results for each of the sections and subsections of this chapter. The objective is to verify, through the local and global Moran indexes consolidated in tables, the results between the measurements through the sensor and their respective counter-evidence tests, and whether these present compliance with the reasonable variation of a maximum error margin of 5%. In this case, an integration factor method was used to determine the relative variation rate between the measurements with the sensor and their respective control test.

$$\int_{0,95}^{1} \frac{df}{dx} = \frac{\sum vl(iref)CRS - \sum vl(iref)CRScp}{1-0,95} \qquad (14)$$

where,

vl(iref)CRS → Reference index value (global and local Moran) of carbon retained in the sink (crop soil, forest soil, crop, and forest);

vl(iref)CRScp → Reference index value (global and local Moran) of the control test of carbon retained in the sink (crop soil, forest soil, crop, and forest).

Table 1. Explanations of the elements of the global Moran index.

Component	Meaning
Moran I statistic standard deviation	Standardized value of the global Moran index, used to test the significance of spatial autocorrelation.
p-value	Probability associated with the hypothesis test, indicating the statistical significance of the observed spatial autocorrelation.
Moran I statistic	Value of the global Moran index calculated for the data, indicating the presence and direction of spatial autocorrelation.
Variance	Moran's index variance, used to calculate the standard deviation and assess the statistical significance of autocorrelation.

Table 2. Explanations of the elements of Moran's local index.

Component	Meaning
Ii (Índice Local de Moran I)	Measures local spatial autocorrelation for each spatial unit (e.g., municipality, neighborhood, pixel). Positive values indicate clustering of similar values, while negative values indicate dispersion (spatial outliers).
E.Ii (Expected Ii)	The expected value of the local Moran index under the null hypothesis (absence of spatial autocorrelation). This value serves as a reference for

	comparison with the observed index.
Var.Ii (li variance)	Measures the variability of the Moran local index, that is, how much the values can fluctuate due to fluctuations in the data. A high variance suggests greater uncertainty in the local index.
Z.Ii (Z-standardized)	Measures how many standard deviations the Ii value is away from the expected value (E.Ii). Higher values indicate stronger spatial patterns. If Z.Ii is very high or very low, it means that the spatial autocorrelation is statistically significant.
Pr (z != E (Ii)) (p-value)	Measures the statistical significance of the local Moran index. A p-value less than 0.05 indicates that the spatial autocorrelation is statistically significant, i.e., it did not occur by chance.

During the 2023/2024 summer harvest, a comparative analysis was carried out between the values of carbon retained in the soil of crops, obtained by sensors and by laboratory control tests, on four rural properties in the state of Paraná. The spatialization of sensory data allowed the construction of thematic maps, which represent in a georeferenced manner the average carbon contents per hectare. This approach allowed a visual and technical assessment of the spatial consistency between the collection methods. The sensory data were represented in georeferenced maps that demonstrate the distribution of the total carbon retained in the soil.

The spatial analysis of the carbon retained in the soil of the crops was performed using the global Moran index (Moran I), which evaluates the spatial autocorrelation of the variables of interest. For this study, measurements of carbon retained in the soil obtained by proprietary sensors and their respective control tests were used. The calculation of the global Moran index was performed from the relative variation rates between these two measurements, as described in equation 14. The analysis was conducted in three steps: (1) calculation of the global Moran index for the sensored measurements, (2) calculation of the global Moran index for the control measurements, and (3) calculation of the global Moran index using the relative variation rate between the sensored and control measurements. The statistical analysis was performed using Moran's I randomization, with the definition of a spatial weight matrix, and the Moran's I values were compared with the expectation and variance of a standard normal distribution. The p-value of each analysis was calculated to determine the significance of the results. The relative variation rate was calculated using equation 1, which integrated the values of carbon retained in the soil of the crops and their counter-evidence.

Results

Retained carbon soil crop and its respective counter-evidence

The percentage variations between the methods for the total carbon retained in the soil, both in the productive areas of the properties (S1 Fig.) and in the counter-evidence areas (S2 Fig.), remained within the maximum limit of 5%, as established by Brazilian national legislation (Brazilian Law 15.042/2024). The percentage differences varied between -5% and 5%, with the following values for the properties: on property 1 - Bela Vista, the variation was -5% (8.33 t/ha in the sensed measurements and 8.78 t/ha in the counterevidence); on property 2 - Pp Socorro, the variation was 5% (7.89 t/ha in the sensed measurements and 7.52 t/ha in the counterevidence); on property 3 - Smart Farm, the variation was -1% (10.39 t/ha in the sensor measurements and 10.47 t/ha in the counter-evidence); and on property 4 - FVanguarda, the variation was 5% (11.06 t/ha in the sensor measurements and 10.51 t/ha in the counter-evidence). These results indicate the accuracy of the sensors in estimating the carbon retained in agricultural soil and reinforce the reliability of the equipment used, demonstrating its technical and legal viability for environmental monitoring and certification in the context of the regulated carbon credit market.

Global Moran's index for carbon retained in the tillage soil and its respective counter-evidence

The results of the global Moran's index for the carbon retained in the tillage soil (Table 3) suggest a possible positive spatial autocorrelation. The same pattern was observed for the counterevidence, with the global Moran's index indicating a possible positive spatial autocorrelation, although the significance was marginally significant. When analyzing the global Moran's index for the relative rate of change between the sensed measurements and their counter-evidence (Table 3), strong spatial autocorrelation was observed. The positive variance of 2.451 suggests stability in the calculations, indicating that the spatial weight matrix was well defined. Based on these results, there is strong evidence of spatial clusters, with regions of the crop soil showing high values next to other high values and low values next to other low values. The significance and positive variances indicate that the spatial pattern is not random.

Table 3. Statistics of Moran's index, of the total carbon retained in the tillage soil, in its respective counter-evidence, and from the relative rate of change between the total carbon retained in the tillage soil and its counter-evidence.

		Farms			
	Elements of the local Moran index	**1**	**2**	**3**	**4**
Carbon retained in tillage soil	Ii	0.928	0.928	0.892	0.892
	E.Ii	-0.220	-0.435	-0.176	-0.502

	Var.Ii	0.687	0.983	0.580	1.000
	Z.Ii	1.385	1.374	1.403	1.395
	Pr (z != E (Ii))	0.166	0.169	0.161	0.163
Carbon retained in the tillage soil counter-evidence	Ii	0.620	0.620	0.873	0.873
	E.Ii	-0.062	-0.689	-0.281	-0.301
	Var.Ii	0.233	0.857	0.809	0.842
	Z.Ii	1.414	1.414	1.284	1.280
	Pr (z != E (Ii))	0.157	0.157	0.199	0.201
Rate of change (Tillage soil vs. Counter-evidence)	Ii	1.447	1.447	1.650	1.650
	E.Ii	0.264	1.050	0.427	0.751
	Var.Ii	0.859	1.719	1.298	1.721
	Z.Ii	2.616	2.606	2.510	2.499
	Pr (z != E (Ii))	0.021	0.021	0.024	2.382

Local Moran's index for carbon retained in tillage soil and its counter-evidence

Analysis of the spatial autocorrelation of carbon retained in tillage soil was carried out using the local Moran's index (Ii) to assess the spatial distribution of carbon data measured by sensors and their counter evidence. The results of the sensor measurements showed Ii values ranging from 0.89 to 0.93, indicating a positive spatial autocorrelation, but without statistical significance, which suggests that the spatial pattern can be considered random (Table 3). Similarly, the counter-evidence showed Ii values between 0.62 and 0.87, also with positive spatial autocorrelation, but without statistical significance ($p > 0.05$), indicating that the spatial pattern in these measurements can also be interpreted as random (Table 3). However, when analyzing the relative rate of change between the sensed measurements and their counter-evidence, the local Moran's index values were higher, ranging from 1.44 to 1.65, indicating a stronger and statistically significant positive spatial autocorrelation (Table 3). The expected local index (E(Ii)) values ranged from 0.26 to 1.05, and the standardized Z-Statistic (Z(Ii)) was between 2.50 and 2.62, confirming the presence of significant spatial clusters, where areas with high carbon values are grouped with others with high values, and the same occurs with areas with low values. These results indicate that although the individual measurements do not show significant spatial autocorrelation, the analysis of the relative rate of change between the sensed data and its counter-evidence reveals a systematic grouping pattern, i.e., spatial clusters of carbon retained in the tillage soil. This suggests a robust conformity between the sensed data and its counter-evidence. Such clustering patterns are statistically significant and indicate that the spatial structure of carbon in tillage soil follows a non-random distribution, with important implications for carbon management, potentially guiding more effective and sustainable agricultural practices (S3 and S4 Fig.).

Carbon retained in the forest soil and its respective counter-evidence

The percentage variations between the retained carbon measurements taken in the forest soil (S5 Fig.) and their respective counter evidence (S6 Fig.) show that, on the properties analyzed, the differences are minimal and within acceptable limits. For example, on the Bela Vista property, the sensed measurement indicated 27.46 tons/ha of retained carbon, while the counter-evidence registered 27.71 tons/ha, with a variation of -1%. On the Pp Socorro property, both values were the same, 29.85 ton/ha, resulting in a 0% variation. At Smart Farm, the values also coincided, with 14.83 ton/ha in both measurements, resulting in 0% variation. The

FVanguarda property, on the other hand, showed a variation of -4%, with 8.95 ton/ha in the sensed measurement and 9.34 ton/ha in the counter-evidence. These results indicate a considerable match between the sensor measurements and the counter-evidence, within the 5% variation limit established by the Brazilian carbon credits regulated market law (Brazilian Law 15.042/2024). It can therefore be said that the sensors used can reliably reflect the amounts of carbon retained in the forest soil, meeting the criteria required by the legislation for the certification of carbon credits. This alignment reinforces the validity of using these sensors as an effective tool for monitoring soil carbon on farms, contributing to the management of carbon sinks and the implementation of carbon credit policies in Brazil.

Global Moran's index for carbon retained in the forest soil and its respective counter-evidence

From the Moran's index statistics for the sensed measurements (Table 4) and the counter-evidence (Table 4), it was observed that the Moran's index statistics were positive for both the sensed data and the counter-evidence, with values of 0.913 and 0.566, respectively. The expectation for Moran's index was negative in both cases (-0.333), which is expected under the hypothesis of no spatial autocorrelation. The observed variance was 0.741 for the sensed data and 0.581 for counter-evidence, indicating that the spatial distribution of the data shows moderate variations, but within acceptable limits. The Moran's I test revealed that although the p-value for both sets of data (sensed and counter-evidence) are slightly above the conventional threshold of 0.05 – both equal to 0.079 – the observed spatial pattern can still be interpreted as non-random, indicating marginally significant spatial autocorrelation.

Table 4. Statistics of Moran's index, of the total carbon retained in the forest soil, in its respective counter-evidence, and from the relative rate of change between the total carbon retained in the forest soil and its counter-evidence.

	Elements of the local Moran index	Farms			
		1	**2**	**3**	**4**
Carbon retained in the forest soil	Ii	0.914	0.914	0.818	0.818
	E.Ii	-0.229	-0.406	-0.131	-0.567
	Var.Ii	0.706	0.965	0.456	0.982
	Z.Ii	1.361	1.344	1.406	1.399
	Pr (z != E (Ii))	0.174	0.179	0.160	0.162
Carbon retained in the forest soil counter-evidence	Ii	0.926	0.926	0.840	0.840
	E.Ii	-0.239	-0.399	-0.141	-0.554
	Var.Ii	0.726	0.960	0.485	0.988
	Z.Ii	1.366	1.353	1.408	1.402
	Pr (z != E (Ii))	0.172	0.176	0.159	0.161
Rate of change (forest soil *vs.* counter-evidence)	Ii	1.828	1.828	1.647	1.647
	E.Ii	0.464	0.800	0.271	1.114
	Var.Ii	1.423	1.912	0.935	1.957
	Z.Ii	2.709	2.679	2.796	2.782
	Pr (z != E (Ii))	0.002	0.002	0.002	0.002

The global Moran's index (Table 4) obtained a Moran's I value of 2.705, indicating strong positive spatial autocorrelation, i.e., areas with high values are close to others with high values and areas with low values are close to others with low values, with a non-random distribution (p-value = 0.0008). In addition, the positive variance of 1.244 indicates that the spatial weight matrix used in the analysis was well defined and stable. These results are consistent with the presence of spatial clusters, i.e., regions where the carbon values retained in the soil are grouped systematically.

Local Moran's index for carbon retained in forest soil and its counter-evidence

Local Moran's index analysis was carried out to assess the spatial autocorrelation of the carbon retained in the forest soil (S7 Fig.), considering both the sensed measurements and the counter-evidence (S8 Fig.). For the sensed data, the Local Moran index values (Ii) ranged from 0.818 to 0.914 (Table 4), indicating a positive spatial autocorrelation. These results suggest that regions with high carbon values are close to each other, as are regions with low values. The expected local index ($E[Ii]$) ranged from -0.406 to -0.229, showing that the observed values are significantly higher than expected under the hypothesis of no spatial autocorrelation. The standardized Z-statistics varied between 1.34 and 1.41, with p-values between 0.160 and 0.179, indicating that, although there is a tendency towards spatial clustering, the statistical significance of the clusters detected is not strong enough to reject the null hypothesis of randomness. For the counter-test data (Table 4), Ii values ranged from 0.840 to 0.926, confirming a positive spatial autocorrelation similar to that of the sensed data. The expected local index ranged from -0.554 to -0.239, suggesting a significant spatial pattern, with most of the observed values well above the expectation under the null hypothesis. The Z-Statistics for the counter-evidence ranged from 1.35 to 1.41, with p-values between 0.159 and 0.176, indicating that, as with the sensed data, the spatial clusters identified are not significant. When the sensed data and the counter-evidence were combined to calculate the local Moran's index from the relative rate of change (Table 4), the Ii values varied between 1.65 and 1.83, reinforcing the presence of a stronger positive spatial autocorrelation. The expected local index ranged from 0.27 to 1.11, and the Z-Statistics increased to values between 2.68 and 2.80, indicating that the observed spatial clusters are more consistent. The p-values, all below 0.05 (ranging from 0.021 to 0.023), indicated that the clusters identified are statistically significant at a 5% level, confirming the presence of robust spatial groupings.

Carbon retained in the crop and its respective counter-evidence

The percentage variations between the measurements sensed in the crop and the respective counter-evidence of retained carbon (S9 and S10 Fig.) show a high degree of agreement between the methods, within the legal parameters established (Brazilian Law 15.042/2024), with variations of up to 5%, which are considered technically acceptable for monitoring and certification in the regulated carbon credit market. On the Bela Vista property, the variation was just 1%, with the sensor measurement indicating 9.08 t/ha and the counter-evidence 9.00 t/ha, showing good precision. The Pp Socorro property showed a slight underestimation of 3%, with the sensor estimating 10.06 t/ha compared to the counter-evidence of 10.38 t/ha. The Smart Farm and FVanguarda properties showed the greatest percentage variation, both with 4%, where the sensors detected 11.24 t/ha and 11.04 t/ha, respectively, while the counter-evidence recorded 10.82 t/ha and 10.60 t/ha.

Global Moran's index for carbon retained from tillage and its respective counter-evidence

The sensed measurements showed a global Moran's index value of 0.663, indicating the presence of positive spatial autocorrelation - that is, the tendency for geographically close areas to have similar values of carbon retained in the soil. However, the associated standardized statistic (1.410) and the respective p-value (0.079) did not reach statistical significance at the 5% level (Table 5), providing only marginal evidence against the null hypothesis of no spatial autocorrelation. For the counter-evidence, Moran's index was only 0.032, with standardized statistics of 1.277 and a p-value of 0.101, showing no statistically significant spatial autocorrelation. This result suggests that the values observed in the counter-proofs do not follow a structured spatial pattern, showing an essentially random distribution in the territory analyzed. When the rate of relative variation between the sensed measurements and their respective counter-evidence was analyzed, a distinct spatial pattern was found: Moran's index was 2.088, with a standardized statistic of 2.074, a p-value of 0.0046, and a variance of 2.072. These values (Table 5) indicate strong and statistically significant positive spatial autocorrelation, revealing the presence of well-defined spatial clusters of relative variations, both for positive and negative discrepancies. This spatial structure reinforces the hypothesis that differences between measurement methods do not occur randomly but are associated with geographical or environmental factors common to the regions where they are concentrated.

Table 5. Statistics of Moran's index, of the total carbon retained in the crop, in its respective counter-evidence, and from the relative rate of change between the total carbon retained in the crop and its counter-evidence.

		Farms			
	Elements of the local Moran index	**1**	**2**	**3**	**4**
Carbon retained in the crop	Ii	0.507	0.507	0.818	0.818
	E.Ii	-0.731	-0.039	-0.352	-0.211

	Var.Ii	0.787	0.150	0.913	0.666
	Z.Ii	1.396	1.409	1.225	1.261
	Pr (z != E (Ii))	0.163	0.159	0.221	0.207
Carbon retained in the plowing counter-evidence	Ii	-0.428	-0.428	0.492	0.492
	E.Ii	-0.952	-0.021	-0.254	-0.106
	Var.Ii	0.183	0.084	0.758	0.378
	Z.Ii	1.225	-1.406	0.857	0.972
	Pr (z != E (Ii))	0.221	0.160	0.392	0.331
Rate of change (crop vs. counter-evidence)	Ii	2.420	2.420	3.387	3.387
	E.Ii	1.547	0.379	0.557	0.291
	Var.Ii	0.891	0.215	1.535	0.960
	Z.Ii	2.409	2.587	1.913	2.052
	Pr (z != E (Ii))	0.031	0.026	0.050	0.044

Local Moran's index for retained carbon and its respective counter-evidence

For the sensed values (S11 Fig.), the *Ii* indexes showed moderate positive values (Table 5), ranging between 0.507 and 0.818, suggesting a tendency for spatial clustering between areas with similar values of retained carbon. The associated theoretical expectations (E[Ii]) were negative or close to zero (between -0.731 and -0.039), and the variances of the indexes varied between 0.150 and 0.913. The resulting standardized Z-statistics were between 1.225 and 1.409, indicating a moderate departure from the null hypothesis of no spatial autocorrelation. However, the corresponding p-values (between 0.159 and 0.221) did not reach statistical significance at the 5% level, which prevents the null hypothesis from being rejected and suggests that the clusters identified can be attributed to chance. Even so, the spatial classification revealed internal consistency: two observations with a Low-Low pattern (low values surrounded by equally low neighbors) and two with a High-High pattern (high values surrounded by high neighbors).

The counter-evidence (S12 Fig.) showed more dispersed Ii values (Table 5), ranging from -0.428 to 0.492. The theoretical expectancies were between -0.952 and -0.021, with variances between 0.084 and 0.758. The Z-statistics oscillated between -1.406 and 1.225, and the p-values ranged from 0.160 to 0.392, characterizing the absence of statistical significance in all cases. Despite this, the spatial patterns observed maintained a certain consistency with those seen in the sensor measurements: the first two observations showed Low-High and High-Low patterns (discrepant values with their neighbors), while the last two preserved the High-High pattern.

The most sensitive and statistically robust approach was the one that considered the relative rate of change between the sensed values and their respective counter-evidence (Table 5). In this configuration, the Ii indexes showed high values (between 2.420 and 3.387), with theoretical expectations ranging from 0.291 to 1.547 and variances between 0.215 and 1.536. The resulting Z-statistics ranged from 1.913 to 2.587, with p-values between 0.026 and 0.050 - all below the 5% threshold, confirming the statistical significance of local spatial autocorrelation. These findings show the existence of significant spatial clusters, i.e., local groupings of similar relative variation between measurement methods. The spatial classification maintained the pattern of the previous analyses: the first two observations were configured as Low-High and High-Low, indicating local discrepancies, while the last two retained the High-High pattern, reaffirming the presence of areas with high spatial consistency in the magnitude of the variations.

Carbon retained in the forest and its respective counter-evidence

On the Bela Vista property, the sensor measurement of carbon retained in the forest indicated 20.03 tons of carbon per hectare (S13 Fig.), while the counter-evidence showed 19.35

tC/ha (S14 Fig.), corresponding to a variation of 3%. The FVanguarda property showed a similar result, with 6.59 tC/ha measured with sensors and 6.38 tC/ha in the counter-proof, also with a variation of 3%. The Pp Socorro property showed a negative difference of -5%, with 21.46 tC/ha from the sensor measurement and 22.46 tC/ha from the counter-proof. Smart Farm showed 10.86 tC/ha in the sensor measurement and 11.25 tC/ha in the counter-proof, resulting in a variation of -4%. All the properties showed variations within the margin of error established by current legislation. According to Brazilian Law 15.042/2024, which establishes guidelines for the regulated carbon credit market in Brazil, the maximum tolerance for divergence between sensory measurements and counterevidence is 5%. Therefore, the results obtained show that the sensors used are technically and operationally compliant, faithfully reflecting the real amounts of carbon retained in the forest sinks of the properties analyzed. The reliability of the data is reinforced by the methodological adjustments described in the correction factors (items F to M, see methods), which ensured the standardization and validation of the measurements. The proximity between the sensed values and the counter-evidence values indicates that the equipment used is effective for quantifying carbon in forest soil, and that it can be used as a valid instrument in the context of carbon credit certification.

Global Moran's index for carbon retained in the forest and its respective counter-evidence

The spatial structure of the carbon retained in the forest soil was assessed using the global Moran's index, considering the sensory measurements, the counter-evidence, and the relative rate of change between the two. Initially, the results of the sensory measurements indicated a Moran's I value of 0.869, with an expectation of -0.333 and a variance of 0.724 (Table 6). The standardized standard deviation was 1.413, resulting in a p-value = 0.079, which does not reach statistical significance at the 5% level, although it does indicate a tendency towards positive spatial autocorrelation.

Table 6. Statistics of Moran's index, of the total carbon retained in the forest, in its respective counter-evidence, and from the relative rate of change between the total carbon retained in the forest and its counter-evidence.

	Elements of the local Moran index	Farms			
		1	**2**	**3**	**4**
Carbon retained in the forest	Ii	0.921	0.921	0.817	0.817
	E.Ii	-0.242	-0.390	-0.129	-0.572
	Var.Ii	0.733	0.952	0.451	0.979
	Z.Ii	1.358	1.344	1.409	1.403
	Pr (z != E (Ii))	0.174	0.179	0.159	0.161
Carbon trapped in the forest counter-evidence	Ii	0.838	0.838	0.752	0.752
	E.Ii	-0.165	-0.473	-0.107	-0.589
	Var.Ii	0.551	0.997	0.381	0.136
	Z.Ii	1.351	1.313	1.391	1.362
	Pr (z != E (Ii))	0.177	0.189	0.164	0.173
Rate of change (forest vs. counter-evidence)	Ii	2.639	2.639	2.353	2.353
	E.Ii	0.356	0.755	0.207	1.016
	Var.Ii	1.124	1.705	0.728	0.976
	Z.Ii	2.371	2.325	2.449	2.420
	Pr (z != E (Ii))	0.044	0.046	0.040	0.042

Similarly, the data from the counter-proofs showed a Moran's I of 0.790, also with a theoretical expectation of -0.333 and a variance of 0.642. The standard deviation was 1.408, with p = 0.0796, reinforcing the indication of positive autocorrelation, although again without statistical significance at the 5% level. However, when considering the rate of relative variation between the sensed values and their respective counter-evidence, as defined by equation 1, with a tolerance of up to 5% difference between measurements, a significantly different spatial pattern was observed. The Moran's index resulting from the consolidation of this data showed a high value of 2.512, with a theoretical expectation of -0.333 and a variance of 1.819. The standardized standard deviation was 1.053, with a p-value = 0.008, highly significant at the 5% level. These results indicate a strong positive spatial autocorrelation in the relative variation data, with robust evidence of systematic clusters of similar values. In practical terms, this means that areas with high relative variation tend to be close to each other, as do regions with low variation. The statistical significance of the test and the positive variance indicate that the spatial weight matrix has been properly defined and that the spatial pattern identified is not random. It can therefore be concluded that the carbon values retained in the forest soil, measured by sensors and validated by counter-evidence, show a coherent and structured spatial pattern. The variation between measurements is within the legally accepted limit of 5%, as stipulated by Brazilian Law 15.042/2024, giving statistical and technical validity to the measurement methodology employed.

Local Moran's index for carbon retained in the forest

In the sensed data, the values of the local Moran's index (Ii) were high (Table 6), standing at 0.921 for the first two properties and 0.817 for the last two (S15 and S16 Fig.). These values indicate strong local clustering of similar values, as predicted by the logic of the index. The associated theoretical expectations (E[Ii]), which serve as a reference under the null hypothesis of no spatial autocorrelation, were negative, ranging from -0.242 to -0.572. The variances of the indexes ranged from 0.451 to 0.979, providing support for the calculation of the standardized Z statistic, whose values were between 1.34 and 1.41. Despite indicating a consistent departure from the expected value, the respective p-values (from 0.159 to 0.179) did not reach statistical significance at the 5% level. Even so, the spatial classification revealed cohesive groupings: High-High patterns in the first two properties and Low-Low patterns in the last two. The counter-evidence showed similar behavior. The Ii indexes varied between 0.752 and 0.838, with theoretical expectations between -0.165 and -0.589 and variances between 0.136 and 0.997. The resulting Z-statistics remained in the range of 1.31 to 1.39, and the p-values, between 0.164 and 0.189, were also not statistically significant. The spatial classification, however, reaffirmed the groupings identified earlier, reinforcing the consistency of the patterns detected, albeit at an exploratory level.

The most robust evidence of spatial autocorrelation emerged from the analysis of the relative rate of change between the sensed values and their counter-evidence. The Ii values in this approach were substantially higher, ranging from 2.353 to 2.639, far exceeding theoretical expectations (E[Ii] between 0.207 and 1.016). The variances remained stable (0.728 to 1.705), and the resulting Z-statistics, between 2.325 and 2.449, showed significant deviations from the expected value under the null hypothesis. Crucially, all the associated p-values were below 0.05 (between 0.040 and 0.046), confirming the presence of statistically significant positive spatial autocorrelation at the 5% level. This demonstrates the existence of well-defined local clusters, in which properties with similar patterns of variation are spatially grouped, highlighting the effectiveness of this approach in revealing latent spatial structures in forest carbon data.

Discussion

The carbon retention values obtained were significant, with total carbon retained in forest per hectare being 14.74 (tCO2e), total carbon retained in crop per hectare being 10.36 (tCO2e), Total carbon retained in forest Soil per hectare being 20.27 (tCO2e) and total carbon retained in crop soil per hectare being 9.42 (tCO2e). These results reveal the effectiveness of the practices adopted and the substantial contribution made by these properties to mitigating climate change. In addition, they confirm measurements with sufficient precision to guarantee compliance with the criteria required by the legislation of the regulated carbon credit market. The methodology developed in this research, which integrates sensors, artificial intelligence, and georeferencing, makes it possible to accurately measure the values needed to sell carbon credits, strengthening the sustainability of the properties and guaranteeing auditable and continuous data for monitoring [21, 22].

The local and global Moran indexes reinforce the fact that geolocation and the management carried out in specific areas directly influence the levels of carbon sequestration on the properties. For both the sensed data and the counter-evidence, significant positive spatial autocorrelation was observed, with the distribution of carbon retained in the forest soil showing non-random patterns and well-defined spatial clusters. The application of spatial analysis based on these indexes reinforces the effectiveness of the methods used to identify geographical patterns of carbon retention, contributing to the reliability of the estimates and making it possible to robustly verify the effectiveness of management practices [23, 24]. Thus, after consolidating the analyses, it can be seen that although the individual data (sensor and counter-evidence) are not statistically significant in isolation, the relative rate of variation between them shows consistent and statistically significant spatial groupings. This indicates that the deviations between measurements maintain an organized spatial structure, which reinforces the reliability of the sensing system as a reflector of the spatial dynamics of carbon retained in crops. This consistency in the results allows us to conclude that, when evaluated based on the relative rate of change between sensory measurements and counter-evidence, the distribution of carbon retained in forest soil displays a non-random and highly structured spatial pattern. The identification of High-High clusters in the first two properties and Low-Low clusters in the last two reinforces the reliability of the sensors in capturing real spatial variations in the distribution of carbon retained in forest soil, within the 5% tolerance limits established by Brazilian Law 15.042/2024. In this sense, it can be said that rural properties can become reliable sources for generating secure carbon credits, provided they adopt technologies, methodologies, and mechanisms that follow the standards established by regulated markets.

However, as is widely observed in the current context, the legal requirements to maintain the preservation of native forests on rural properties have not been enough to guarantee the effective conservation of green areas [25, 26, 27]. Although enforcement and fines are important, they have not been entirely effective in preventing deforestation and forest degradation. In this sense, the use of remuneration mechanisms, such as carbon credits based on regulated market standards, is a promising alternative, encouraging more sustainable management, guaranteeing the preservation of forests, and promoting the recovery of degraded areas [28].

According to [14], it is argued that carbon credit project initiatives and their use in offsetting emissions represent an “authorization to pollute” and do not contribute to reducing emissions. Although this criticism is relevant and should be considered in the global debate, it does not invalidate the mechanisms when implemented with technical rigor. If linked to precise measurements, independent audits, and robust methodologies, as proposed in this research, carbon credits can represent effective instruments for the transition to a low-carbon economy. The technology developed here allows credits to be generated based on concrete evidence and georeferenced data, rewarding real CO_2 reductions throughout the life cycle of production systems [29].

Another important point addressed in this research, based on data from the World Bank [30], is that sectors such as oil and gas, steel, mining, logistics, and manufacturing account for around 50% of the world's GDP. If these industries zeroed their emissions exclusively through internal reductions, without the possibility of buying carbon credits, they would face a critical situation, with around half of the global economy coming to a standstill. This analysis highlights the urgent need for complementary mechanisms, such as the purchase of carbon credits from projects that use methodologies such as the one proposed by this research, to ensure that economic sectors can continue their operations while looking for viable ways to reduce their emissions [31, 32, 33, 34]. Therefore, the results achieved in this research demonstrate that the use of secure carbon credit mechanisms, backed by regulated market standards, offers a transitional solution to reduce emissions while maintaining standing forests and agricultural areas [35]. This approach allows companies in heavy economic sectors, which face great difficulties in reducing their emissions immediately, to offset their emissions until they become capable of implementing technologies for carbon reduction in a financially viable way. The proposed methodology provides a solid basis for the generation and certification of certified carbon credits, ensuring that the transition to a low-carbon economy takes place in a gradual, scalable, and sustainable manner [36, 37].

On the international stage, there is a historical inequality between the northern hemisphere, which has concentrated on the benefits of economic growth based on emissions, and the southern hemisphere, which currently has vast potential for carbon removal through forests and agricultural areas [38, 39]. Mechanisms such as the one proposed here allow for the creation of financial and environmental bridges between these regions, enabling countries to acquire removal credits generated in regions with a natural vocation for carbon sequestration. In addition to mitigating the impacts of climate change, this arrangement promotes social and economic benefits in the regions that produce the credits, strengthening climate justice and contributing to equity between countries at different stages of economic and technological development [40, 41].

Conclusions

The research reveals the capacity of rural properties, especially those with forested areas, to capture carbon from the atmosphere, as well as highlighting the importance of adopting sustainable management to maximize this potential. The use of strategies aimed at recovering degraded soils, reducing production costs, and increasing carbon removal capacity shows a new way to optimize the yield of these properties, combining production and sustainability.

When monetized through carbon credits, following the strict standards of regulated markets, rural properties become fundamental pillars for the preservation of native forests, transforming them into robust sources of carbon retention. The adoption of advanced technologies and methodologies to recover degraded areas makes it possible to simultaneously meet the growing demand for food and effectively combat greenhouse gas emissions, without the need for deforestation.

By integrating the carbon credits generated by rural properties into regulated markets, an effective mechanism is established for the preservation and recovery of forest areas. This approach has emerged as one of the most powerful solutions for mitigating the global climate crisis, placing rural properties as key players in the fight for environmental sustainability.

Acknowledgements

Thanks to the Agricultural Engineering Program at Unioeste in the person of Professor Miguel Angel Uribe Opazo for their support in the development of the research. Thanks to CAPES for the research grant, without which it would not have been possible to achieve the results of this research. Thanks to NetWord Operações Agrícolas for providing me with the hours I needed to take part in this research.

References

1. Wang A, Fang Y, Gurmesa GA. Potential of land-based terrestrial carbon sinks to mitigate climate change. In: European Geosciences Union General Assembly 2024 (EGU24); 2024 Apr 14-19; Vienna, Austria. Available from: https://doi.org/10.5194/egusphere-egu24-2264.
2. Lennon J, Barrett B. Conserving an underappreciated heritage resource: The rural landscape. Parks Stewardship Forum. 2024;40(3).
3. Dulal HB, Brodnig G, Shah KU. Capital assets and institutional constraints to implementation of greenhouse gas mitigation options in agriculture. Mitig Adapt Strateg Glob Change. 2011;16(1):1-23.
4. Feng Y. Research on the legal guarantee for realizing the goal of "Dual Carbon" in rural areas. Adv Econ Manag Res. 2024;12(1):668-673.
5. Kutter A, Westby LD. Managing rural landscapes in the context of a changing climate. Dev Pract. 2014;24(4):544-558.
6. Gupta S, Kumar M, Priyadarshini R. Electrical conductivity sensing for precision agriculture: A review. In: Yadav N, Yadav A, Bansal J, Deep K, Kim J, editors. Harmony search and nature inspired optimization algorithms. Advances in intelligent systems and

computing. Singapore: Springer; 2019. Available from: https://doi.org/10.1007/978-981-13-0761-4_62.

7. Asner GP, Powell GV, Mascaro J, Knapp DE, Clark JK, Jacobson J, Kennedy-Bowdoin T, Balaji A, Paez-Acosta G, Victoria E, Secada L, Valqui M, Hughes RF. High-resolution forest carbon stocks and emissions in the Amazon. Proc Natl Acad Sci U S A. 2010;107(38):16738-16742.
8. Sipthorpe A, Brink S, Van Leeuwen T, Staffell I. Blockchain solutions for carbon markets are nearing maturity. One Earth. 2022;5(7):779-791.
9. Ma W, Qiu H, Rahut D. Rural development in the digital age: does information and communication technology adoption contribute to credit access and income growth in rural China? Rev Dev Econ. 2022;27(3):1421-1444.
10. White A, Lutz D, Howarth R, Soto J. Small-scale forestry and carbon offset markets: an empirical study of Vermont current use forest landowner willingness to accept carbon credit programs. PLoS One. 2018;13(8):e0201967.
11. Poudyal N, Bowker J, Siry J. Factors influencing buyers' willingness to offer price premiums for carbon credits sourced from urban forests. Int J Sustain Soc. 2015;7(3):205.
12. Tan H, Zhang Q. Application of blockchain hierarchical model in the realm of rural green credit investigation. Sustainability. 2021;13(3):1324.
13. Balmford A, Brancalion PHS, Coomes D, Filewod B, Groom B, Guizar-Coutiño A, et al. Credit credibility threatens forests. Science. 2023;380(6644):466-467.
14. Pande R. Can the market in voluntary carbon credits help reduce global emissions in line with Paris Agreement targets? Science. 2024;384(6696).
15. Ferronato MAF, Silva SV, Silva Neto AJ. Modelagem de objetos e algoritmo de distribuição de sensores para uma ferramenta computacional visando aplicações em agricultura de precisão. Cereus. 2019;11(1).

16. Ferronato MAF, Silva SV, Silva Neto A. Modelagem de objetos para uma ferramenta computacional em agricultura de precisão para distribuição maximizada de sensores de aquisição dos atributos de solos por proximidade. Cereus. 2018;10(2):86-100.
17. R Development Core Team. R: A language and environment for statistical computing. Vienna, Austria: R Foundation of Statistical Computing; 2021. Available: http://www.r-project.org.
18. QGIS Development Team. QGIS Geographic Information System. 2023. Available from: https://qgis.org/.
19. Google Cloud Platform. The new shape of the cloud starts here. 2025. Available from: https://cloud.google.com/.
20. Instituto Nacional de Pesquisas Espaciais. Brasília, 2025. Available from: https://www.gov.br/inpe/pt-br.
21. Segaran RB, Rum SN, Ninggal MI, Aris TNM. Efficient ML technique in blockchain-based solution in carbon credit for mitigating greenwashing. Discov Sustain. 2025;6:281.
22. Brown S. Measuring, monitoring, and verification of carbon benefits for forest-based projects. Philos Trans A Math Phys Eng Sci. 2002;360(1797):1669-83.
23. Bassam S, Osman N, Haitham S. New methods for analyzing spatio-temporal simulation results of Moran’s index. J Comput Eng Inf Technol. 2018;7(2).
24. Fu WJ, Jiang PK, Zhou GM, Zhao KL. Using Moran's I and GIS to study the spatial pattern of forest litter carbon density in a subtropical region of southeastern China. Biogeosciences. 2014;11:2401–2409.
25. Ima CGV, Giles A, Espírito Santo MM, Mesquita RCG, Vieira DLM, Massoca P, et al. Governance and policy constraints of natural forest regeneration in the Brazilian Amazon. Restor Ecol. 2025;33(1):e14272.

26. Laudares SSA, Borges LAC, Rezende JLP, Bicalho ML, Barros VCC. New contours of the native vegetation protection law of 2012. Floresta Ambient. 2019;26(4):e20160612.

27. Rodrigues RJ, Ondaera GK, Kobal MB, Bergamasco MC. Impacts on the environmental landscape caused by alterations in the new Forest Code. Appl Res Agrotechnol. 2014;7(3).

28. Mendieta D, Grueso JR. Bonos de carbono como alternativas para luchar contra la deforestación en Colombia. Veredas Dir. 2024;21:e212666.

29. Mendieta D, Grueso JR. Bonos de carbono como alternativas para luchar contra la deforestación en Colombia. Veredas Dir. 2024;21:e212666.

30. World Bank Open Data. Free and open access to global development data. Available from: https://data.worldbank.org/.

31. Kopytin I. Carbon credits in decarbonization strategies of oil and gas companies. World Econ Int Relat. 2024;68(11):84-92.

32. Anukwonke C, Abazu C. Green Business through Carbon Credit. In: Climate Change Alleviation for Sustainable Progression: Floristic prospective and arboreal avenues as a viable sequestration tool. Dervash MA, Wani AA, editors. 1 st ed. Boca Raton: CRC Press; 2022. Available from: https://doi.org/10.1201/9781003106982

33. Okedele P, Aziza R, Oduro P, Ishola A. Carbon pricing mechanisms and their global efficacy in reducing emissions: lessons from leading economies. Res J Eng Technol. 2024;7(2):114-25.

34. van Sluisveld MAE, Boer HS, Daioglou V, Hof AF, van Vuuren DP. A race to zero: assessing the position of heavy industry in a global net-zero CO_2 emissions context. Energy Clim Change. 2021;2:100051.

35. Adhisankaran K, Manivannan V, Sakthivel N, Balachandar D, Ragunath K, Vasumathi V. Agricultural carbon credits: a pathway to environmental sustainability. Plant Sci Today. 2024;11(4).

36. Al Mazrouei S, Aggarwal DK, Ganesan S, Kumaravel R. Leveraging carbon market mechanism to achieve de-carbonization targets [presentation]. Abu Dhabi, UAE: ADIPEC; October 2023. DOI: 10.2118/216539-MS.

37. Raymond L. Carbon trading. In: Elgar encyclopedia of climate policy. Fiorino DJ, Eisenstadt TA, Ahluwalia, MK, editors. Cheltenham: Edward Elgar Publishing; 2024. Available from: https://doi.org/10.4337/9781802209204.ch62.

38. Box EO. Vegetation analogs and differences in the Northern and Southern Hemispheres: a global comparison. Plant Ecol. 2002;163:139-54.

39. Sovacool BK. Expanding carbon removal to the Global South: thematic concerns on systems, justice, and climate governance. Energy Clim Change. 2023;4:100103.

40. Tan KC. Climate reparations: why the polluter pays principle is neither unfair nor unreasonable. WIREs Clim Change. 2023;14(4):e827.

41. Jouzel J. Climate change and climate justice. In: Laurent É, editor. The well-being transition. Singapure: Springer; 2021. p. 13-23. Available from: https://doi.org/10.1007/978-3-030-67860-9_2.

Supporting information

S1 Fig. Georeferenced map of the total carbon retained in the soil of the properties' crops.

S2 Fig. Georeferenced map of the counter-evidence of the total carbon retained in the soil of the properties' crops.

S3 Fig. Georeferenced map of the local Moran's index of the carbon retained in the soil of the farms.

S4 Fig. Georeferenced map of the local Moran's index of carbon retained in the soil of the farms.

S5 Fig. Georeferenced map of the carbon retained in the forest soil of the properties.

S6 Fig. Georeferenced map of the counter-evidence of the carbon retained in the forest soil of the properties.

S7 Fig. Georeferenced map of the local Moran's index of carbon retained in the soil of the forest properties.

S8 Fig. Georeferenced map of the local Moran's index of carbon retained in the forest soil of the properties.

S9 Fig. Georeferenced map of the carbon retained from the properties' crops.

S10 Fig. Georeferenced map of the counter-evidence of retained carbon from the properties' crops.

S11 Fig. Georeferenced map of the local Moran's index of the carbon retained in the farms' crops.

S12 Fig. Georeferenced map of the counter-evidence of the local Moran's index of the carbon retained in the farms' crops.

S13 Fig. Georeferenced map of the retained carbon of the forest of the properties.

S14 Fig. Georeferenced map of the counter-evidence of the retained carbon of the forest of the properties.

S15 Fig. Georeferenced map of the local Moran's index of the retained carbon of the forest of the properties.

S16 Fig. Georeferenced map of the local Moran's index of retained carbon in the forest of the properties.

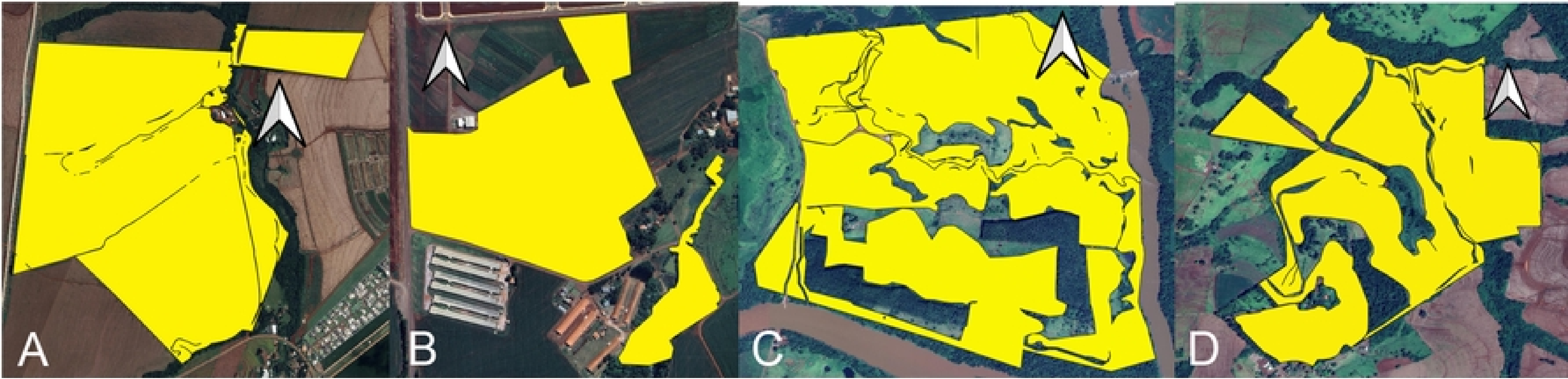

Figure